⌘ *Author's Choice*

THE JOURNAL OF BIOLOGICAL CHEMISTRY VOL. 284, NO. 23, pp. 15867–15879, June 5, 2009

A Family of Bacterial Cysteine Protease Type III Effectors Utilizes Acylation-dependent and -independent Strategies to Localize to Plasma Membranes*[S]

Received for publication, January 26, 2009, and in revised form, March 16, 2009 Published, JBC Papers in Press, April 3, 2009, DOI 10.1074/jbc.M900519200

Robert H. Dowen[‡§], James L. Engel[‡], Feng Shao[‡1], Joseph R. Ecker[¶2], and Jack E. Dixon[‡‖3]

From the [‡]Departments of Pharmacology, Cellular and Molecular Medicine, and Chemistry and Biochemistry, the [§]Biomedical Sciences Graduate Program, and [‖]The Howard Hughes Medical Institute, University of California, San Diego, La Jolla, California 92093-0721 and the [¶]Plant Biology Laboratory, The Salk Institute for Biological Studies, La Jolla, California 92037

Bacterial phytopathogens employ a type III secretion system to deliver effector proteins into the plant cell to suppress defense pathways; however, the molecular mechanisms and subcellular localization strategies that drive effector function largely remain a mystery. Here, we demonstrate that the plant plasma membrane is the primary site for subcellular localization of the *Pseudomonas syringae* effector AvrPphB and five additional cysteine protease family members. AvrPphB and two AvrPphB-like effectors, ORF4 and NopT, autoproteolytically process following delivery into the plant cell to expose embedded sites for fatty acylation. Host-dependent lipidation of these three effectors directs plasma membrane localization and is required for the avirulence activity of AvrPphB. Surprisingly, the AvrPphB-like effectors RipT, HopC1, and HopN1 utilize an acylation-independent mechanism to localize to the cellular plasma membrane. Although some AvrPphB-like effectors employ acylation-independent localization strategies, others hijack the eukaryotic lipidation machinery to ensure plasma membrane localization, illustrating the diverse tactics employed by type III effectors to target specific subcellular compartments.

Plants have evolved sophisticated mechanisms to recognize invading bacterial pathogens and, upon infection, can coordinate an extremely efficient defense response. Detection of microbes occurs rapidly through recognition of a variety of nonspecific elicitors, or microbe-associated molecular patterns, that trigger a basal nonspecific resistance response that is often sufficient in controlling most invading bacteria (1). However, phytopathogens including *Pseudomonas syringae*, *Xanthomonas campestris*, *Erwinia amylovora*, and *Ralstonia solanacearum* employ a type III secretion system (TTSS)[4] to deliver an arsenal of virulence proteins (effectors) into host cells that suppress basal defenses and render the plant susceptible to disease (2). *P. syringae* pv. *tomato* DC3000, for example, secretes ~30 effectors into the plant cell that are responsible for defining host specificity and, as a collection, are indispensable for disease progression (3, 4).

However, resistant plants have developed mechanisms to defend against effector function and specifically recognize a given pathogen. These plants initiate a potent defense response that is often characterized by a localized programmed cell death reaction, or hypersensitive response (HR), at the site of infection, which often occurs concomitantly with cessation of pathogen growth (5). Although the underlying signaling molecules involved in HR induction are only beginning to be uncovered, it is clear that HR progression is dependent on plant disease resistance (*R*) gene products that specifically recognize bacterial effector avirulence (Avr) proteins (6). The simplest model for initiation of R protein defenses requires a direct protein-protein interaction between the bacterial Avr protein and the host R protein; however, only a handful of these "gene-for-gene" interactions have been uncovered (7–9). Recent studies also support a model for an indirect recognition event whereby an effector biochemically alters a host protein, which in turn is sensed by a single downstream R protein or multiprotein complex (2). In this case, R proteins are responsible for "guarding" against manipulation of a host protein by an Avr effector protein.

The molecular mechanisms that dictate R protein activation in the large part remain a mystery; however, biochemical and functional data for a few Avr-R protein relationships have underscored the importance of subcellular localization in transducing plant defenses. The two archetypal examples of effectors whose functions are defined by specific subcellular localizations are the *P. syringae* Avr proteins AvrB and Avr-

* This work was supported, in whole or in part, by National Institutes of Health Grant AI060662 (to J. E. D.) and Pharmacology Training Grant 2 T32 GM07752-25 (to R. H. D.).

⌘ *Author's Choice*—Final version full access.

[S] The on-line version of this article (available at http://www.jbc.org) contains supplemental Figs. S1–S7 and additional "Experimental Procedures."

[1] Current address: National Institute of Biological Sciences, Beijing 102206, China.

[2] To whom correspondence may be addressed. Tel.: 858-453-4100 (ext. 1795); Fax: 858-558-6379; E-mail: ecker@salk.edu.

[3] To whom correspondence may be addressed: 9500 Gilman Dr., La Jolla, CA 92093-0721. Tel.: 858-822-0491; Fax: 858-822-5888; E-mail: jedixon@ucsd.edu.

[4] The abbreviations used are: TTSS, type III secretion system; AvrPphB, avirulence gene *Pseudomonas syringae* pv. *phaseolicola* B; ORF4, open reading frame 4; NopT, nodulation outer protein T; RipT, *Ralstonia* effector injected into plant cells T; HopC1, Hrp outer protein C1; HopN1, Hrp outer protein N1; YopT, *Yersinia* outer protein T; PBS1, AvrPphB susceptible 1; RPS5, resistant to *Pseudomonas syringae* 5; PIP2A, plasma membrane intrinsic protein 2A; HR, hypersensitive response; *R* gene, resistance gene; R protein, resistance protein; Avr, avirulence; YFP, yellow fluorescent protein; CFP, cyan fluorescent protein; PM, plasma membrane; *Pst*, *Pseudomonas syringae* pv. tomato DC3000; *Pf*, *Pseudomonas fluorescens*; *PR1*, pathogenesis-related gene 1; cfu, colony forming unit; HA, hemagglutinin epitope; NPTII, neomycin phosphotransferase II; h.p.i., hours post-infection; NMT, *N*-myristoyl transferase; PAT, palmitoyl acyltransferase.

Rpm1, which both localize to host plasma membranes where they initiate R protein defenses (10). Interestingly, mislocalization of AvrB or AvrRpm1 abolishes their avirulence activities (10). These data emphasize the importance of proper effector localization in the host cell and allude to the fact that other type III effectors may employ similar strategies to promote their function.

We have previously shown that the *P. syringae* pv. *phaseolicola* effector AvrPphB is a member of the YopT family of cysteine proteases and specifically cleaves the *Arabidopsis* protein kinase PBS1 to initiate *RPS5*-dependent HR (11, 12). Consistent with the guard model, PBS1 forms a protein complex with plasma membrane-localized RPS5 in "anticipation" of proteolytic cleavage by AvrPphB (13, 14). Upon delivery into the host cell, AvrPphB autoproteolytically processes to reveal a novel amino terminus containing putative sites for both *N*-myristoylation and *S*-palmitoylation (10, 15). Although AvrPphB appears to interact with membranes through the putative myristoylation site (10), there has been no biochemical evidence supporting fatty acylation of AvrPphB, and to date it remains unclear if lipidation of AvrPphB is necessary for cleavage of PBS1 and subsequent HR induction *in planta*.

In this study, we have identified additional AvrPphB family members, utilized by evolutionary diverse phytopathogens, which remarkably possess autoprocessing activity. Cleavage, in turn, reveals embedded sites for fatty acylation that are post-transcriptionally modified by the eukaryotic machinery *in vivo*. Consequently, host lipidation of these AvrPphB-like effectors ensures plasma membrane localization. We demonstrate that acylation of AvrPphB is absolutely required for cleavage of PBS1 and induction of *RPS5*-dependent defenses at the plant plasma membrane. Surprisingly, some AvrPphB family members do not autoprocess and, in turn, are not acylated. Nonetheless, these effectors localize to plasma membranes using acylation-independent strategies. Together, these studies illustrate the complex tactics employed by type III effectors to localize within specific subcellular compartments, thereby enhancing their effective concentrations and likely promoting their biological function.

EXPERIMENTAL PROCEDURES

Plasmids and Pathogen Strains—All PCR-based cloning was performed using standard procedures and all point mutations were generated using the QuikChange Site-directed Mutagenesis kit (Stratagene) using the manufacturer's instructions. Effector cDNAs were cloned from genomic DNA: *P. syringae* pv. *phaseolicola* (ATCC 11355D), *P. syringae* pv. *tomato* DC3000 (isolated using standard procedures), *R. solanacearum* GMI1000 (gift from Timothy Denny), and *Rhizobium* sp. NGR234 cosmid pXB740 (16). cDNAs were cloned into the mammalian expression vector pcDNA3.1 (Invitrogen) for *in vitro* transcription/translation experiments, into the yeast expression vector pRS425-GAL (gift from Richard Kolodner) for *Saccharomyces cerevisiae* experiments, and into the plant 35S cytomegalovirus expression vector pCHF3-YFP for localization studies (17). *avrPphB* and *orf4* alleles were expressed behind their native promoters in *P. syringae* pv. *tomato* DC3000 (gift from Brian Staskawicz) or *Pseudomonas fluorescens* pLN1965 (gift from James Alfano) using the broad host-range plasmid pVSP61 (18). The *P. fluorescens* pLN1965 strain is identical to *P. fluorescens* pLN18 (19) but allows for use the pVSP61 plasmid encoding kanamycin resistance. The pVSP61::*avrPphB* plasmid has been described previously (20). The *orf4* gene (200 bp upstream and 400 bp downstream) was cloned into pVSP61. All pVSP61 plasmids were introduced into *Pseudomonas* strains (grown on KB media at 28 °C) via triparental mating using a DH5α helper strain carrying the plasmid pRK2013. The *AtPBS1* genomic clone was isolated from Col-0 genomic DNA as described previously (11), tagged with a 3× HA epitope directly upstream of the stop codon, and cloned into the binary vector pJHA212B. The resulting vector was transformed into *pbs1-1* (21) plants via *Agrobacterium*-mediated floral dipping and T_1 *pbs1-1*:*PBS1-HA* plants were isolated by Basta selection in soil.

In Vitro Autoprocessing Assays—Effectors in pcDNA3.1 were *in vitro* transcribed and translated in wheat germ extract (Promega) in the presence of [^{35}S]methionine (Amersham Biosciences) according to manufacturer's instructions. At the specified time points, 5 μl of the total reaction volume (50 μl) were removed, quenched in 2× SDS sample buffer, subjected to SDS-PAGE, and analyzed by autoradiography.

Protein Purification for Edman Degradation—Recombinant effector proteins were partially purified from *E. coli* lysates (see supplemental "Experimental Procedures" for details) and Edman degradation was performed by the University of California at San Diego Protein Sequencing Facility.

Yeast in Vivo Labeling—In vivo labeling of *S. cerevisiae* was performed as previously described with modifications (22). Briefly, C-terminal 2× FLAG-tagged effectors were expressed under a galactose-inducible promoter (pRS425-GAL) in the protease-deficient RDKY1293 strain (MATα, *ura3–52*, *trp1*Δ*63*, *leu2*Δ*1*, *his3*Δ*200*, *pep4*::*HIS3*, *prb1*Δ*1.6R*, *can1*, *GAL*; gift from R. Kolodner). Yeast strains grown to mid-log phase in YPAD were diluted (5:50 ml) into complete minimal media containing 3% raffinose and grown to stationary phase. Approximately 1.7×10^9 cells were then resuspended in 100 ml of rich media (1% Bacto Yeast Extract, 2% Bacto Peptone, and 4% galactose) and grown for 4 h at 30 °C. Cells ($\sim 1 \times 10^9$) were resuspened in 25 ml of rich media containing 3% galactose, 3 μg/ml cerulenin (Sigma), and 30 μCi/ml [^{3}H]myristic acid or 50 μCi/ml [^{3}H]palmitic acid (PerkinElmer Life Sciences). Yeast were labeled for 4 h at 30 °C before harvesting. Cell lysis and protein immunoprecipitation has been described previously (22). For this study, pre-equilibrated anti-FLAG M2-agarose resin (100 μl) was added to the Protein A-agarose (Invitrogen) precleared lysate and rotated overnight at 4 °C. The immunoprecipitations were washed extensively with lysis buffer and eluted with 2× SDS sample buffer. Samples were subjected to SDS-PAGE and the gel was treated with Amplify (Amersham Biosciences) to enhance the tritium signal before drying. The gel was analyzed by autoradiography ([^{3}H]myristic acid, 1-month exposure; [^{3}H]palmitic acid, 10-month exposure). To determine protein expression, identical samples were analyzed by Western blotting with an anti-FLAG M2 peroxidase conjugate antibody (Sigma).

Total Yeast Membrane Fractionation and Chemical Treatments—Strains were grown to saturation in YPAD before dilution (1:10 ml) into complete minimal media containing 2% raffinose and 0.25–2% galactose (concentration was varied based on protein expression levels). Cells were grown for 8 h and ~1.7×10^8 cells were harvested. Cells were resuspended in 300 mM sorbitol, 100 mM NaCl, 5 mM $MgCl_2$, 10 mM Tris-HCl, pH 7.4, and protease inhibitor tablets (Roche) before addition of acid-washed glass beads (Sigma). Cell disruption was carried out by vigorous vortexing and cell debris was removed by centrifugation at 500 × *g* for 10 min at 4 °C, giving the "total" fraction. The soluble fraction was separated from the insoluble membrane fraction by ultracentrifugation at 100,000 × *g* for 1 h. The membrane pellet was resuspended in lysis buffer containing 1% Triton X-100 to completely solubilize the membranes. Equal volumes (80 μl) of each fraction were added to 20 μl of 5× SDS sample buffer, subjected to SDS-PAGE, and analyzed by Western blotting (anti-FLAG M2, Sigma F1804). A duplicate blot was probed with a monoclonal anti-v-H-Ras antibody (Oncogene Research Products) to detect the yeast plasma membrane marker Ras1p.

Total membranes for chemical treatment experiments were isolated as described above except total lysate was split in 5 equal volumes before ultracentrifugation. Membrane samples were resuspended in lysis buffer, or 1 M NaCl and 10 mM Tris-HCl (pH 7.4), or 2 M urea and 10 mM Tris-HCl (pH 7.4), or 0.1 M Na_2CO_3 (pH 11.5), or 1% Triton X-100 and 10 mM Tris-HCl (pH 7.4) and incubated for 1 hr on ice. Samples were re-fractionated by ultracentrifugation and equal volumes of soluble and insoluble fractions were subjected to SDS-PAGE and Western blot analysis.

Transformation of Chinese Cabbage and Microscopy—Chinese cabbage (*Brassica campestris* subsp. *napus* var. *pekinensis*) leaf slices were transformed by particle bombardment using a Biolistic PDS-1,000/He particle delivery system (Bio-Rad). Gold particles (1.0 μm) were coated with the individual 35S::*effector*-YFP (pCHF3-YFP) or 35S::*AtPIP2A*-CFP (pCHF1-CFP) plasmids according to the manufacturer's instructions. The tissue was bombarded twice using 1,100 p.s.i. rupture discs under a vacuum of 26 inches of mercury. After a 9-h incubation at 22 °C, epidermal peels were imaged using a Zeiss Axiovert microscope (Carl Zeiss Microimaging, Inc.) equipped with a MicroMax digital camera (Roper-Princeton Instruments) controlled by MataFluor software (Universal Imaging, Corp.).

Plant HR and Bacterial Growth Assays—*Arabidopsis thaliana* plants were grown in a Promix-HP:vermiculite (2:1) soil mixture under a 9-h photoperiod at 22 °C. HR assays were performed in 4–6-week-old plants by syringe infiltration of bacteria (~3.75×10^7 cfu ml^{-1}) as previously described (11). Plants were photographed and scored for HR 16–20 h.p.i. for *P. syringae* pv. *tomato* DC3000-treated plants or 45 h.p.i. for *P. fluorescens*-treated plants. *P. syringae* growth assays were performed by dipping 2-week-old seedlings in bacteria (~2.5×10^7 cfu ml^{-1}) exactly as previously described (23). Data are represented as the mean ± S.E. of the decimal logarithm (log[cfu mg^{-1} fresh weight]) of four replicates.

In Planta PBS1 Cleavage Assay—T_2 *pbs1-1*:*PBS1-HA* plants were inoculated with *P. syringae* (3.75×10^7 cfu ml^{-1}) strains by syringe infiltration. Tissue from three independent plants was harvested 14 h.p.i. and homogenized in lysis buffer containing 20 mM Tris-HCl (pH 7.4), 150 mM NaCl, 1 mM EDTA, 5 mM dithiothreitol, 1% Triton X-100, and 2× plant protease inhibitor mixture (Sigma). Lysate was cleared by centrifugation at 10,000 × *g* for 5 min and protein concentrations were determined with Bradford reagent (Bio-Rad). Total protein (10 μg) was subjected to SDS-PAGE and Western blot analysis using an anti-HA.11 monoclonal antibody (Covance).

Secretion of AvrPphB Effectors by P. syringae—*P. syringae* strains were grown in KB media to mid-log phase before resuspending the bacteria at an A_{600} of 0.3 in Hrp-inducing minimal media (pH 6.0) containing 10 mM fructose as previously described (24). An overnight-induced (22 °C) 40-ml culture was centrifuged (4,300 × *g*, 15 min) and 20 ml of the supernatant was re-centrifuged for 40 min at 17,200 × *g*. 10 ml of the resulting supernatant was removed and protein was precipitated with 11.5% trichloroacetic acid, washed with acetone, and resuspended in 2× SDS sample buffer. Cell-bound fractions (bacterial pellet) and secreted fractions (supernatant protein, 7.5-fold concentrated) were subjected to SDS-PAGE and probed with a polyclonal anti-AvrPphB antibody (whole serum, 1:10,000) or a polyclonal anti-Neomycin Phosphotranserase II antibody (Upstate). Antisera was generated against recombinant AvrPphB(Δ62)-His_6 protein (11) in rabbit (Cocalico Biologicals).

Induction of PR1 Expression—Two-week-old plants were infected by dipping (~2.5×10^7 cfu ml^{-1}) and aerial tissue from 4–5 plants (one biological replicate) was collected 24 h.p.i. RNA was isolated using the RNeasy plant mini kit (Qiagen) and cDNA was generated from total RNA (1 μg) using the Superscript III kit (Invitrogen) and oligo(dT) primers according to the manufacturer's instructions. qPCR were run on a MX4000 Multiplex QPCR machine (Stratagene) using a Power SYBR Green PCR Mastermix kit (Applied Biosystems). Primer pairs for *PR1* (target) and *TUA3* (endogenous control) have been previously described (25). C_t values were generated using default parameters and relative expression values were calculated using $2^{-\Delta\Delta Ct}$. Data presented are the mean ± S.E. of the fold-change in *PR1* transcript compared with mock (no bacteria) of at least 5 biological replicates (comprised of three technical replicates) from two independent experiments.

RESULTS

Identification of an AvrPphB-like Effector Subfamily within the YopT Family of Cysteine Proteases—Bioinformatic analyses of the YopT family suggest that more than 30 evolutionary diverse bacterial organisms utilize putative cysteine protease virulence factors to promote disease in animal, marine, or plant species (supplemental Fig. S4) (12). Using PSI-BLAST (26), we searched for novel AvrPphB family members from recently sequenced plant pathogens or symbiotes that were identical to AvrPphB at the Cys/His/Asp catalytic residues, as well as the invariant residues Tyr-105 and Pro-228 (numbered from the AvrPphB sequence). Thirteen sequences from different bacterial strains were identified, and the full-length proteins were aligned using the BLOSUM matrix. Although residues surrounding the catalytic amino acids are heavily conserved, similarity outside of these

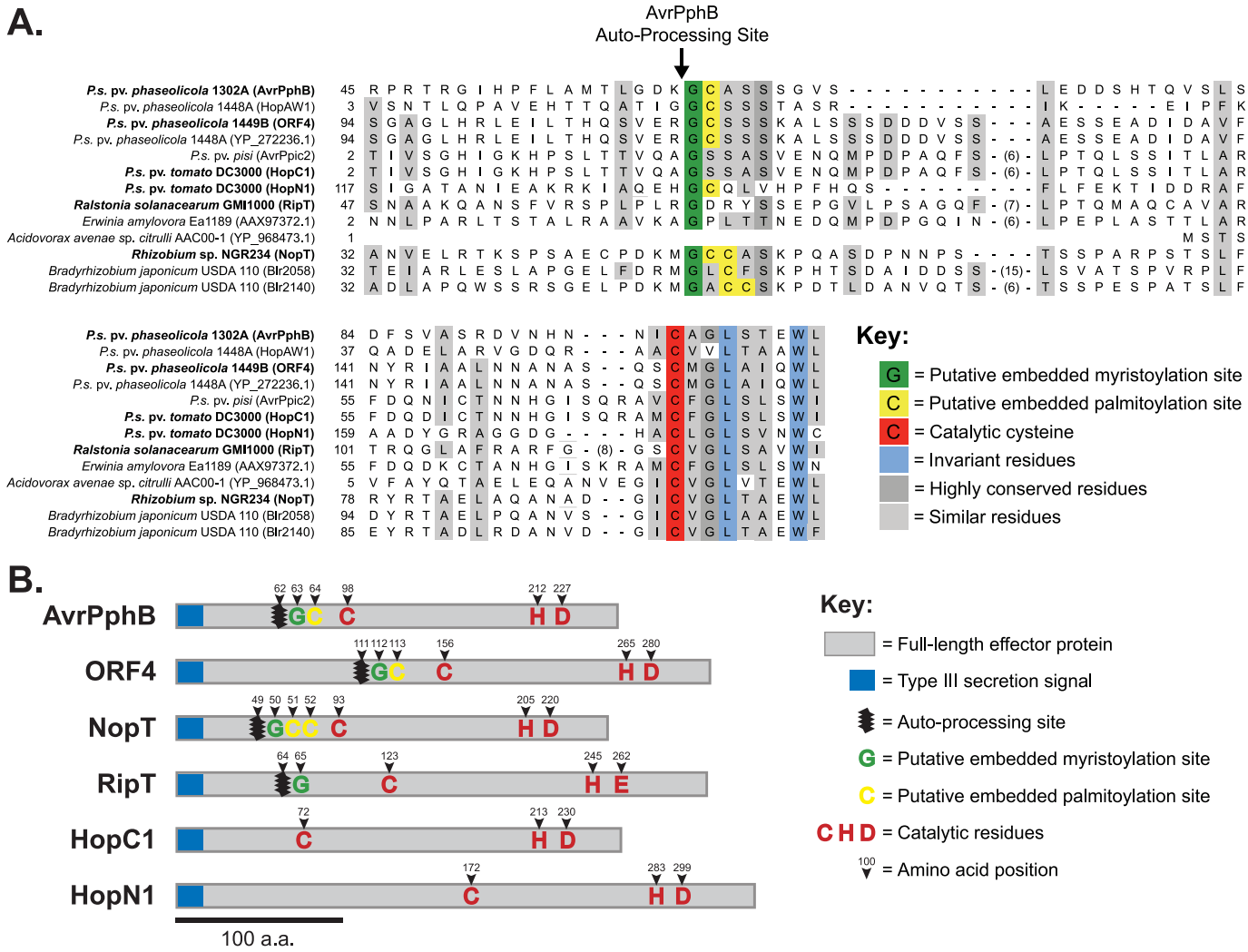

FIGURE 1. **Multiple amino acid sequence alignment of the AvrPphB family reveals conserved residues within the NH_2 terminus.** *A*, members of the AvrPphB family were identified by PSI-BLAST using the AvrPphB sequence as the query and the amino termini were aligned. The full alignment is displayed in supplemental Fig. S1. Residues that share homology, as well as the catalytic cysteine and the embedded acylation sites, are colored according to the key. The known autoprocessing site in AvrPphB is also indicated (Shao *et al.* (12) and Puri *et al.* (15)). Proteins examined in this study are in *bold*. Additional accession numbers are as follows: AvrPphB, Q52430; HopAW1, AAX12112; ORF4, AAD47206; AvrPpic2, CAC16701; HopC1, AAO54131; HopN1, AAO54892; RipT, NP_521333; NopT, AAB91961; Blr2058, NP_768698; Blr2140, NP_768780. *B*, a schematic of the full-length effector proteins examined in this study. The catalytic residues, autoprocessing sites, and acylation sites are displayed according to the key.

regions is extremely limited (supplemental Fig. S1). Surprisingly, all AvrPphB-like effector proteins are predicted to have a secondary structure (using psipred) similar to that of the known AvrPphB structure (27), suggesting that these proteins have been evolutionarily tailored by the bacteria to maintain cysteine protease activity, but likely target different host proteins. Surprisingly, we also identified a conserved patch of residues in the amino terminus of the AvrPphB family members that comprise an embedded consensus site for eukaryotic fatty acylation (Fig. 1*A*), implying that proteolytic processing of these effectors at specific residues may generate functional eukaryotic lipidation motifs.

AvrPphB Family Members Self-process at Specific Residues within the NH_2 Terminus—The *P. syringae* pv. *phaseolicola* effector AvrPphB is a 35-kDa protein that self-proteolytically processes into a 28-kDa mature protein, requiring the Cys/His/Asp catalytic triad for this unique activity (Fig. 1*A*) (12, 15). We examined five additional AvrPphB family members (Fig. 1*B*), from evolutionary diverse pathogens, for self-processing activity using an *in vitro* cleavage assay. Interestingly, three other AvrPphB-like effectors (ORF4, NopT, and RipT) self-cleaved into ~28 kDa proteins when they were expressed in wheat germ extract (Fig. 2*A*). Autoproteolytic processing requires the catalytic cysteine, suggesting that the *orf4*, *nopT*, and *ripT* genes encode functional cysteine proteases. Additionally, we observed a more rapid processing of AvrPphB compared with the other effectors in the context of this assay, suggesting that the structure of AvrPphB or the chemical composition of the internal cleavage site is better suited for autoprocessing activity compared with that of ORF4, NopT, and RipT. Surprisingly, the two effectors HopC1 and HopN1 do not autoprocess *in vitro*. Furthermore, self-processing was not detected by Western blot analysis when HopC1 or HopN1 were expressed in *S. cerevisiae* (Fig. 4*A*) or in *A. thaliana* (supplemental Fig. S2), eliminating the possibility that a eukaryotic "activator" is required for processing.

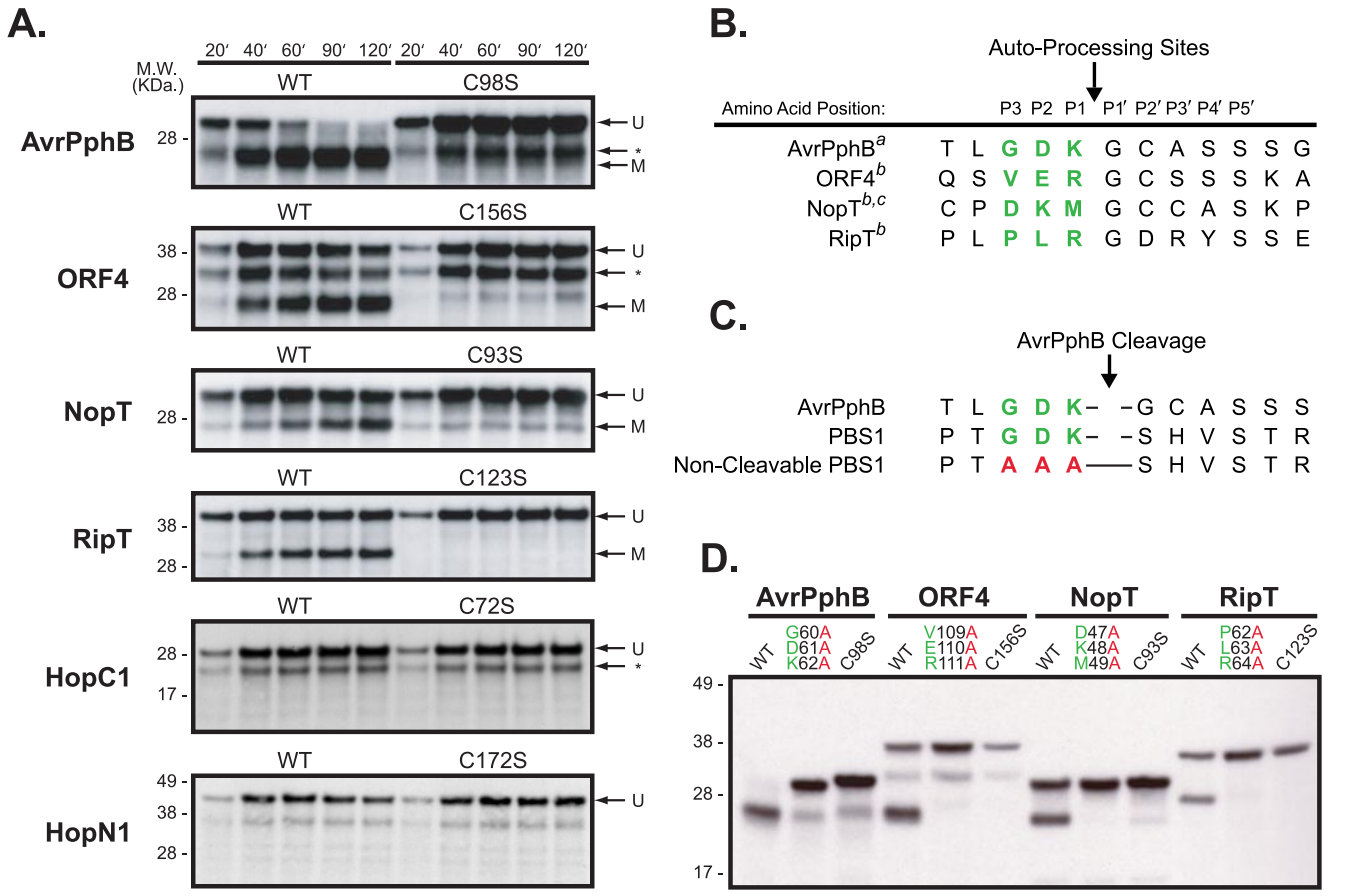

FIGURE 2. **Additional AvrPphB family members undergo autoproteolytic cleavage at specific residues.** *A*, the indicated proteins were *in vitro* transcribed and translated in the presence of [^{35}S]methionine and aliquots were removed at the indicated time points. The samples were subjected to SDS-PAGE and proteins were visualized by autoradiography (Unprocessed proteases, *U*; mature proteases, *M*). Secondary start methionines produce additional protein species during translation (*asterisks*) that generate the following proteins: *AvrPphB*, M = 22 kDa and * (from Met-57) = 23 kDa; *ORF4*, M = 23 kDa and * (from Met-51) = 30 kDa; *HopC1*, U = 29 kDa and * (from Met-29) = 26 kDa. The experiment was performed three times with similar results. *B*, the autoprocessing sites of the mature recombinant proteins were determined by Edman degradation (footnote a data from Puri *et al.* (15); footnote b data from this study; footnote c data from Dai *et al.* (47)). The three residues that precede the cleavage site are shown in *green*. *C*, sequence alignment of the known autoproteolytic processing site in AvrPphB and the cleavage site in PBS1 with the three conserved amino acids that precede the cleavage sites shown in *green*. Mutation of these residues to alanine (*red*) in PBS1 inhibits cleavage by AvrPphB (Shao *et al.* (11)). *D*, the indicated P1/P2/P3 triple mutants were generated and analyzed as described in *A*. Residues that allow autoproteolytic processing are shown in *green* and mutant residues that prevent cleavage are colored in *red*. The catalytically inactive mutants (C/S) are deficient in autoprocessing activity. Additional protein species generated from secondary start methionines (AvrPphB and ORF4) are as described in *A*. Each experiment was repeated twice with similar results.

To determine the sites of autoproteolytic cleavage, we expressed full-length, COOH-terminal epitope-tagged proteins in *Escherichia coli*, purified the proteins from lysates, and determined their cleavage sites by Edman degradation. ORF4, NopT, and RipT were efficiently processed in bacteria and sequencing revealed that self-cleavage occurs prior to a glycine found in the P1′ position (Fig. 2*B*). Interestingly, self-cleavage of AvrPphB, as well as cleavage of its substrate, PBS1, occurs proximal to a GDK motif that is found in both sequences (Fig. 2*C*). Mutation of all three GDK residues in PBS1 completely inhibits cleavage (11), suggesting that the P1, P2, and P3 residues may be important for effector self-processing. We found that triple mutation of the P1–3 residues in AvrPphB, ORF4, NopT, and RipT prevents self-cleavage (Fig. 2*D*), indicating that these residues are required for recognition and subsequent autoproteolysis of the amino terminus.

Self-proteolysis of AvrPphB-like Effectors Exposes Post-translational Lipid Modification Sites—It has been proposed that autoproteolytic processing of AvrPphB generates sites for fatty acylation (10); however, there is no direct biochemical evidence supporting *N*-myristoylation or *S*-palmitoylation of AvrPphB or any additional family members. We aligned the amino termini of the processed AvrPphB-like effectors and found conserved glycine (P1′) and serine (P5′) residues in AvrPphB, ORF4, and NopT (Fig. 3*A*) that are consistent with the myristoylation consensus sequence (28). All three effectors also possess potential sites for cysteine palmitoylation. Interestingly, RipT, as well as the non-processed effectors HopC1 and HopN1, lack amino-terminal acylation consensus sites and are therefore unlikely to be lipidated.

To determine whether the AvrPphB family members are *N*-myristoylated, we *in vitro* transcribed and translated full-length effector proteins in the presence of [^{3}H]myristic acid. Radiolabeled myristate was efficiently incorporated into AvrPphB, ORF4, and NopT self-processed proteins (supplemental Fig. S3). Myristoylation of these effectors require autoprocessing activity to expose the embedded myristoylation site, as well as the P1′ glycine modification site, because

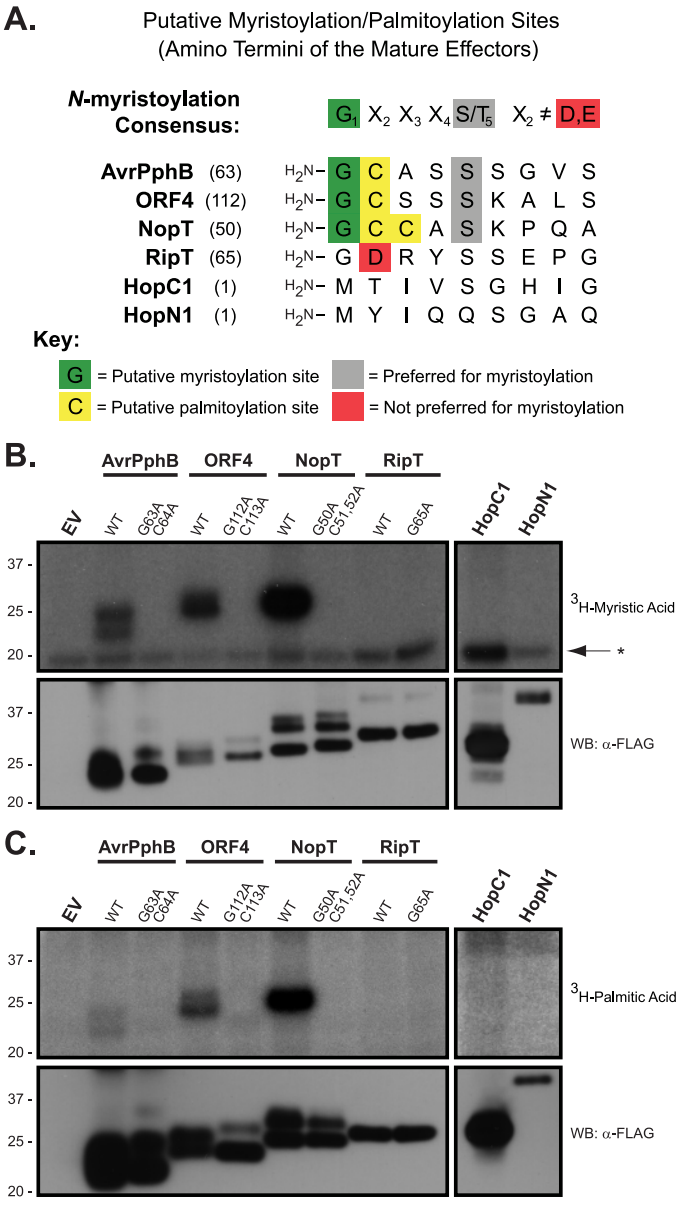

FIGURE 3. **Autoproteolytic processing of AvrPphB family members results in *N*-myristoylation and *S*-palmitoylation of the new amino terminus.** *A*, the NH_2-terminal sequences of the autoprocessed, mature proteins were examined for eukaryotic acylation consensus sites. Important residues are colored according to the key. The myristoylation consensus sequence is based on previous experiments (Utsumi *et al.* (28)). Full-length wild-type and mutant effectors were expressed in *S. cerevisiae* in the presence of 30 μCi/ml [^{3}H]myristic acid (*B*) or 50 μCi/ml [^{3}H]palmitic acid (*C*). After labeling for 4 h, the FLAG-tagged effectors were immunoprecipitated, subjected to SDS-PAGE, and analyzed by autoradiography (*top panel*) or Western blotting with an anti-FLAG antibody (*bottom panel*). An *asterisk* indicates nonspecific bands. Yeast radiolabeling experiments were performed twice with similar results.

the C/S and G/A mutants are not lipidated (supplemental Fig. S3). To examine myristoylation of AvrPphB family members in a cellular system, we expressed the effectors in *S. cerevisiae* in the presence of [^{3}H]myristic acid. Consistent with the *in vitro* studies, AvrPphB, ORF4, and NopT are myristoylated in yeast and acylation is dependent on the P1′ glycine residue (Fig. 3*B*). RipT, HopC1, and HopN1 do not possess myristoylation consensus sites and were not modified. In eukaryotic systems *N*-myristoylation of proteins often occurs concomitantly with *S*-palmitoylation of nearby cysteines, a post-translational modification that enhances membrane association of lipidated proteins (29). To determine whether AvrPphB family members can be palmitoylated by the eukaryotic machinery, we expressed the effectors in *S. cerevisiae* in the presence of [^{3}H]palmitic acid. AvrPphB, ORF4, and NopT, which each possess cysteines proximal to the myristoylation site, are palmitoylated in yeast (Fig. 3*C*). However, the myristoylation-deficient mutants (GC/AA) are likewise not palmitoylated. These mutants are likely not palmitoylated due to either loss of the myristoyl moiety that often initiates subsequent palmitoylation or mutation of the cysteine modification sites. Interestingly, the acylated effectors generally lack any additional putative *S*-palmitoylation sites outside of the *N*-terminal motif (AvrPphB, 3 additional cysteines; ORF4, 1 cysteine; NopT, 0 cysteines; supplemental Fig. S1), and all additional cysteines are positioned in the catalytic core and are unlikely candidates for lipidation. Therefore, it is probable that palmitoylation occurs proximal to the myristoylation sites found in AvrPphB, ORF4, and NopT. These data represent the first direct biochemical evidence for dual acylation of AvrPphB family members and suggest that lipidation by the eukaryotic host machinery may play an important role in effector function.

Interestingly, the AvrPphB family members are not uniformly autoprocessed or lipidated. To investigate if the acylated effectors are evolutionary distinct from the non-acylated effectors, we generated a YopT phylogenetic tree and searched for trends in the autoprocessing or lipidation phenomena (supplemental Fig. S4*A*). The acylated proteins (AvrPphB, ORF4, and NopT) cluster into a common clade that is distinct from the non-acylated effectors (RipT, HopC1, and HopN1), suggesting that an evolutionary division from a common protease ancestor may have given rise to the lipidation feature. Alternatively, the autoprocessing activity of HopC1 and HopN1 and the lipidation sites in RipT may have been lost to redirect localization of these effectors in their respective hosts. We scanned all the remaining untested AvrPphB family members for embedded myristoylation consensus sites, and found putative sites for both *N*-myristoylation and *S*-palmitoylation in the sequences of four additional effectors (Blr2058, Blr2140, HopAW1, and YP_272236, which is identical to ORF4; supplemental Fig. S4*B*). Although these putative lipidation sites lack experimental validation, it is notable that these effectors phylogenetically cluster with the known acylated effectors (supplemental Fig. S4*A*).

The Acylated and Non-acylated AvrPphB-like Effectors Are Differentially Associated with the Plasma Membrane—Traditionally, dual acylation of eukaryotic proteins with myristoyl and palmitoyl moieties directs proteins to cellular membranes, often plasma membranes, where they are oriented into the cytoplasmic face of the lipid bilayer. To test if autoprocessing and subsequent lipidation promotes membrane attachment of AvrPphB family members, we expressed the effectors in *S. cerevisiae* and performed biochemical subcellular fractionation experiments. The acylated effectors AvrPphB, ORF4, and NopT co-fractionate with yeast membranes and the farnesylated Ras1p plasma membrane marker (Fig. 4*A*). Furthermore, these associations require functional acylation sites because the

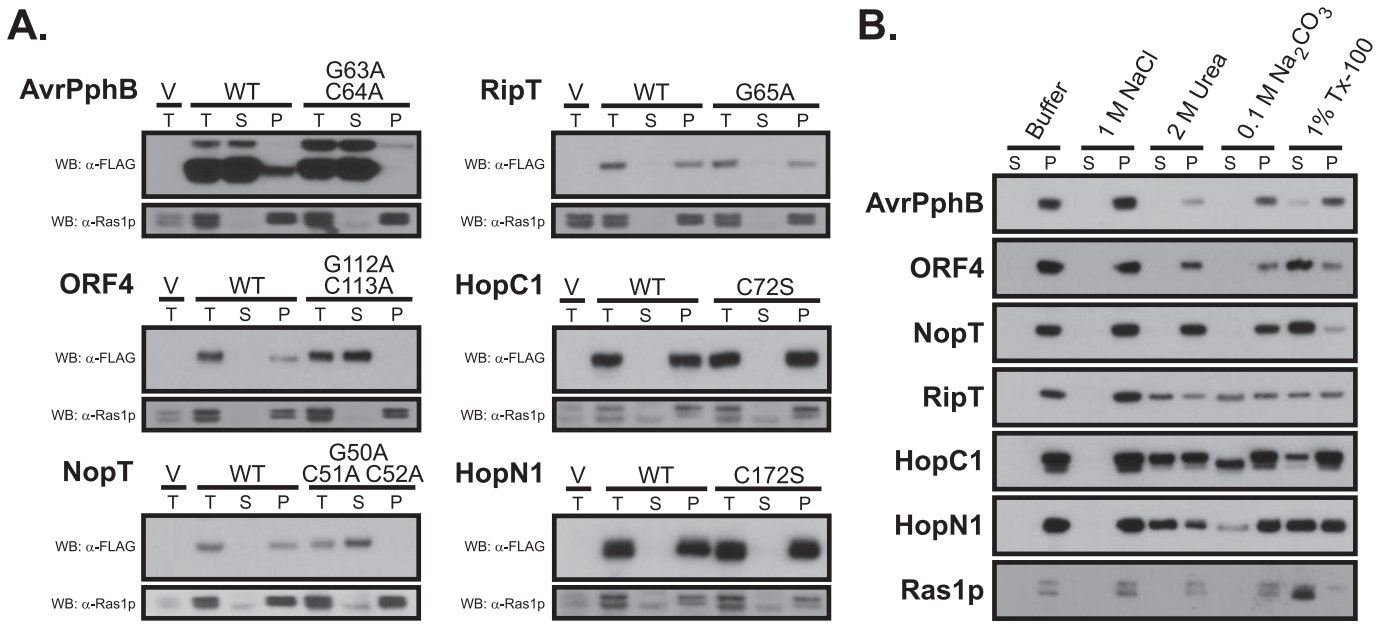

FIGURE 4. **Acylated and non-acylated AvrPphB family members are differentially associated with *S. cerevisiae* membranes.** *A*, strains carrying the indicated FLAG-tagged effectors or empty vector (*V*) were induced with galactose for 8 h and homogenized. Total extracts (*T*) were fractionated into soluble (*S*) fractions and insoluble membrane pellets (*P*) by ultracentrifugation at 100,000 × *g*. Equal volumes of each fraction were subjected to SDS-PAGE, blotted, and probed with anti-FLAG or anti-v-H-Ras (plasma membrane marker) antibodies. *B*, membranes were isolated as in *A* and resuspended in control lysis buffer, high salt buffer (1 M NaCl, 10 mM Tris-HCl, pH 7.4), denaturing buffer (2 M urea, 10 mM Tris-HCl, pH 7.4), high pH buffer (0.1 M Na_2CO_3, pH 11.5), or buffer containing detergent (1% Triton X-100, 10 mM Tris-HCl, pH 7.4). Treated samples were re-ultracentrifuged and equal volumes of the soluble (*S*) and pellet (*P*) fractions were subjected to SDS-PAGE and Western blot (*WB*) analysis as in *A*. Each experiment was performed twice with similar results.

GC/AA mutants localize exclusively to the soluble fraction. We also observed significantly higher expression levels of AvrPphB protein, but a smaller proportion of membrane-associated AvrPphB protein, compared with the other acylated effectors. These data, as well as the modest amounts of [^{3}H]myristic acid and [^{3}H]palmitic acid incorporated into AvrPphB (Fig. 3, *B* and *C*), indicate that lipidation of AvrPphB in *S. cerevisiae* occurs slowly compared with ORF4 and NopT. Differential lipidation rates between effectors are likely a consequence of the chemical context of the residues surrounding the acylation sites and the substrate selectivity of the eukaryotic acylation machinery; however, it is clear that AvrPphB, ORF4, and NopT are all capable of being acylated at the GC motif and are subsequently localized to cellular membranes.

Surprisingly, the non-acylated effectors RipT, HopC1, and HopN1 also fractionate to the insoluble membrane fraction. We observed localization of the RipT P1′ glycine mutant (G65A), as well as the HopC1 and HopN1 catalytically inactive mutants (C/S), exclusively in the membrane fractions, further substantiating that these effectors associate with membranes independent of lipidation. To eliminate the possibility of artifacts of the yeast expression system, we expressed RipT, HopC1, and HopN1 in *Arabidopsis* and performed similar membrane fractionation experiments. Identical results were observed *in planta* (supplemental Fig. S5), indicating that the non-acylated AvrPphB-like effectors are likely *bona fide* membrane proteins.

The membrane fractionation experiments indicate that the acylated and non-acylated AvrPphB-like effectors employ different mechanisms for membrane association and possibly possess different membrane binding affinities. To evaluate the effector-membrane association, we treated yeast membranes with high salt, denaturing, alkaline, or detergent-containing buffers. As expected, the acylated effectors can only be extracted with detergent as exemplified by the farnesylated Ras1p protein (Fig. 4*B*), suggesting lipidation is the predominant component responsible for membrane association. In contrast, the non-acylated effectors are partially extracted with urea, alkaline buffer, and detergent. Although the mechanisms of membrane attachment for the non-lipidated effectors remains unclear, these data suggest that the AvrPphB-like effectors utilize different strategies to localize to membranes and possess different membrane binding affinities.

An overwhelming majority of dual acylated eukaryotic proteins are preferentially localized to plasma membranes (PM) rather than endomembranes (29). To further investigate the cellular localization of the AvrPphB family members, we transiently expressed yellow fluorescent protein (YFP)-tagged effectors in Chinese cabbage epidermal cells and examined localization by fluorescence microscopy. AvrPphB, ORF4, and NopT exhibit a clear plasma membrane localization that is indistinguishable from the *Arabidopsis* PM marker PIP2A (Fig. 5). In contrast, expression of the acylation-deficient mutants generates an unmistakable cytoplasmic localization that is identical to the soluble YFP control staining. Consistent with the biochemical fractionation data, RipT is largely enriched in plasma membranes via an acylation-independent mechanism, because localization of the G65A mutant is identical to that of the wild-type protein. Additionally, the non-lipidated effectors HopC1 and HopN1 are enriched in the plasma membranes of Chinese cabbage cells (Fig. 5). Interestingly, we observed a unique punctate staining of HopN1 in the plasma membranes of Chinese cabbage cells, as well as tobacco epidermal cells (data not shown), which was absent in the additional effectors

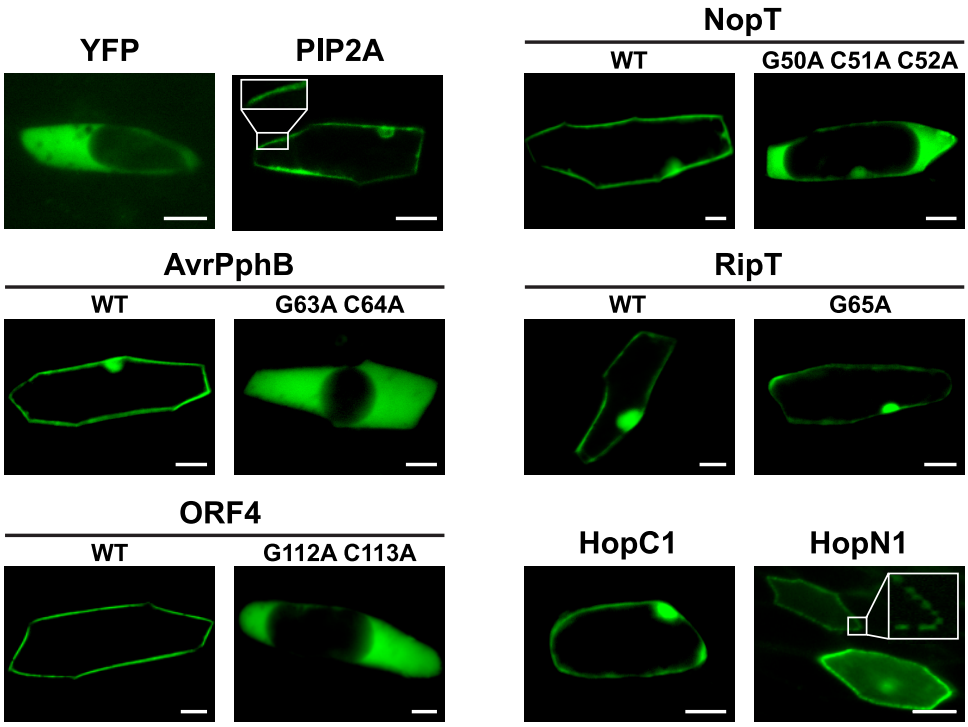

FIGURE 5. **AvrPphB-like family members localize to the plasma membranes of Chinese cabbage cells.** COOH-terminal-tagged YFP effector proteins were transiently expressed in Chinese cabbage epidermal cells using particle bombardment. Representative fluorescent images of cells expressing wild-type effectors or acylation-deficient mutants are indicated. Control bombardments were performed using the cytosolic YFP or plasma membrane-localized PIP2A (plasma membrane intrinsic protein 2A)-CFP proteins. Both YFP and CFP fluorescence are colored in *green*. *Bar*, 50 μm.

and the PIP2A PM marker (Fig. 5, *inset panels*), suggesting that HopN1 may target to a lipid microdomain. It is notable that we observed strong nuclear staining in a large proportion of cells expressing both the wild-type and mutant effectors; however, we also observed this phenomena in cells expressing the known plasma membrane protein PIP2A (Fig. 5), suggesting that overexpression of proteins in this system likely results in nuclear localization artifacts. Although we cannot completely eliminate the possibility that some or all the AvrPphB-like effectors localize to endomembranes at low levels, additional sucrose gradient purification of plasma membranes from *S. cerevisiae* crude membrane fractions revealed that all the wild-type effectors are strongly enriched in the plasma membrane (data not shown). Collectively, these data implicate the plasma membrane as a crucial site for localization of AvrPphB family members and suggest that proper plasma membrane localization may be important for directing effectors to their respective substrates.

The Acylated AvrPphB-like Effectors Possess Distinct Substrate Specificity—The lipidated AvrPphB-like effectors employ identical strategies to ensure plasma membrane localization; however, it is unknown if localization alone is sufficient to direct substrate specificity. AvrPphB proteolytically cleaves the *Arabidopsis* PBS1 protein to initiate HR (11, 13), and it is possible that additional AvrPphB-like effectors target PBS1. To investigate if the acylated effectors are functionally equivalent, we exogenously expressed ORF4, which has the highest similarity to AvrPphB among all the family members (processed proteins: 45% similar, 27% identical), under control of its native promoter in the plant pathogen *P. syringae* pv. *tomato* DC3000 (*Pst*) and verified its expression by reverse transcriptase-PCR and Western blot analysis (data not shown). We inoculated resistant *Arabidopsis* plants with the avirulent *Pst*(*avrPphB*) strain or the *Pst*(*orf4*) strain at high bacterial densities to produce a visually scorable HR-associated tissue collapse. The virulent *Pst*(empty vector) pathogen produces no HR 20 h post-infection; however, *Pst*(*avrPphB*) induces a striking tissue collapse phenotype in 93% of the infected leaves (Fig. 6*A*). Interestingly, strains carrying *orf4* fail to generate a HR. To ensure that the endogenous repertoire of *Pst* effectors is not interfering with ORF4 function, we also performed HR assays using *P. fluorescens* (*Pf*) strains carrying the same effector alleles. Consistent with the *Pst* infections, the *Pf*(*avrPphB*) strain, but not *Pf*(*orf4*), generated a weak, but reliable HR (37 of 59 infected leaves, Fig. 6*A*). Furthermore, recombinant ORF4 protein has no activity against PBS1 in an *in vitro* cleavage assay (supplemental Fig. S6). Together, these data demonstrate that plasma membrane targeting alone is not sufficient to cleave PBS1, and suggest that the acylated AvrPphB-like effectors possess different substrate specificity.

Dual Acylation of AvrPphB Is Required for Cleavage of PBS1 and Initiation of Defenses in Resistant Arabidopsis Plants—Our subcellular localization studies provide strong evidence that AvrPphB is driven to the host plasma membrane by eukaryotic acylation. Interestingly, we have also observed lipidation of PBS1 and RPS5 (data not shown), and additionally, RPS5 associates with *Arabidopsis* membranes (14). Together, these data suggest that PBS1 likely co-localizes with RPS5 at the plasma membrane to guard against AvrPphB; however, it remains unclear if acylation of AvrPphB is required for cleavage of PBS1 and subsequent HR induction.

Cleavage of PBS1 by AvrPphB can be observed *in planta* when both components are overexpressed (11); however, overexpression of the soluble AvrPphB mutant protein in transgenic plants (DEX::*avrPphB GC/AS*) results in an acylation-independent HR that is likely due to overwhelming expression levels in the plant cell (supplemental Fig. S7). To circumvent these overexpression artifacts and ensure proper cellular localization, we performed *in planta* PBS1 cleavage experiments at near endogenous expression levels using *Pst*-delivered AvrPphB proteins and transgenic plants carrying a *PBS1-HA* genomic clone. Partial cleavage of PBS1 occurs in plants inoculated with the *Pst*(*avrPphB*) strain; however, the PBS1 protein is unaffected when strains delivering the acylation-deficient effectors are used (G63A, C64S, and GC/AS, Fig. 6*B*). To ensure

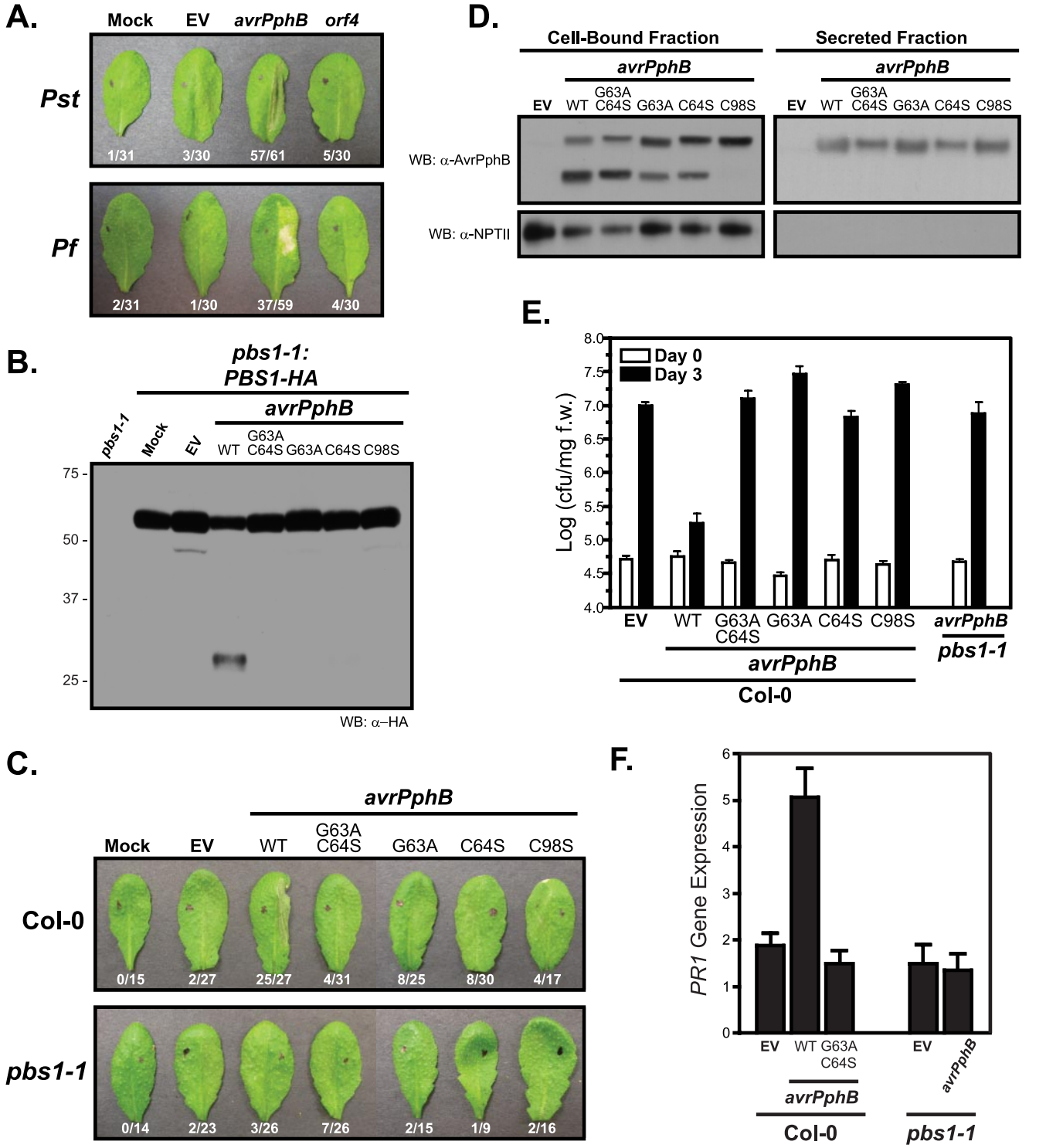

FIGURE 6. **Host acylation of AvrPphB is required for avirulence activity in *Arabidopsis* plants carrying *PBS1*.** *A*, adult Col-0 leaves were syringe infiltrated (opposite to the marked leaf half) with ~3.75 × 10^7 cfu/ml *P. syringae* pv. *tomato* DC3000 (*Pst*) or *P. fluorescens* pLN1965 (*Pf*) strains expressing AvrPphB or ORF4. Also, plants were inoculated with 10 mM $MgCl_2$ (*Mock*) or strains carrying the pVSP61 empty vector (*EV*). Ratios *below* each leaf indicate the number of HR positive leaves/total number of leaves inoculated. *B*, transgenic *pbs1–1*:*PBS1-HA* plants were inoculated as in *A* with the indicated *Pst* strains. Leaf tissue was harvested 14 h.p.i., homogenized, and 10 μg of total protein was subjected to SDS-PAGE. Blots were analyzed by anti-HA Western blotting (*WB*). Three individual T_2 plants were assayed for each infection condition and produced identical results. *C*, Col-0 or *pbs1-1* plants were inoculated as described in *A* with *Pst* strains carrying the indicated *avrPphB* alleles (Gly-63, myristoylation site; Cys-64, palmitoylation site; Cys-98, catalytic cysteine). Data were collected 20 h.p.i. and are representative of two independent experiments. *D*, *Pst* strains carrying the indicated alleles were grown in Hrp-inducing minimal media. Cultures were partitioned into cell-bound and secreted fractions by centrifugation. Protein samples were subjected to SDS-PAGE, blotted, and probed with antibodies against AvrPphB or NPTII (control for nonspecific lysis). *E*, *Arabidopsis* seedlings were inoculated by dipping with *Pst* strains (~2.5 × 10^7 cfu/ml) carrying the indicated effector alleles. At day 0 (*white bars*) or day 3 (*black bars*) the bacteria were extracted and quantified. Data are represented as the mean ± S.E. of four technical replicates. The experiment was repeated twice with similar results. *F*, *Arabidopsis* seedlings were inoculated as described in *E* with the indicated *Pst* strains. Tissue was harvested 24 h.p.i. and RNA was subjected to reverse transcriptase-qPCR analysis using *PR1* and *TUBULIN3* specific primers. *PR1* mRNA levels (relative to *TUB3*) were calibrated to mock-treated samples ($2^{-\Delta\Delta Ct}$). Data are represented as the mean ± S.E. of at least 5 biological replicates from two independent experiments.

that the acylation-deficient mutant is only impaired in subcellular localization and not the intrinsic protease activity, we performed *in vitro* cleavage assays and found the AvrPphB GC/AS mutant to be equally efficient as the wild-type protein in cleaving PBS1 (supplemental Fig. S6).

To determine whether lipidation of AvrPphB is required for efficient HR induction, we inoculated resistant (Col-0) or susceptible (*pbs1-1*) plants with *Pst* strains carrying the wild-type or mutant alleles and performed HR assays. AvrPphB function is severely reduced in resistant plants by mutation of either the myristoylation site (G63A, 32% responding) or palmitoylation site (C64S, 27% responding) when compared with the wild-type protein (25 of 27 leaves or 93% responding, Fig. 6*C*). Mutation of both acylation sites thoroughly diminishes the avirulence activity (13% responding). The AvrPphB mutants were markedly deficient in their ability to generate HR despite the fact that they were all properly delivered through the TTSS as full-length proteins (Fig. 6*D*).

To further examine the role of acylation in promoting the avirulence function of AvrPphB, we tested the ability of the AvrPphB acylation-deficient mutants to suppress growth of the virulent *Pst* DC3000 strain in *Arabidopsis*. As expected, expression of AvrPphB in *Pst* ensures avirulence and limits bacterial growth in resistant (Col-0), but not susceptible (*pbs1-1*) plants (Fig. 6*E*). The acylation-deficient single and double mutants, however, are all defective in avirulence function because these strains grow in Col-0 to similar levels as the virulent *Pst*(empty vector) strain.

Local and systemic defense against the virulent *Pst* pathogen, as well as some avirulent pathogens, requires accumulation of salicylic acid and modulation of salicylic acid-responsive genes for a maximal resistance response (30). Therefore, we examined expression levels of the salicylic acid-inducible gene *PR1* (pathogenesis-related gene 1) in plants 24 h after infection with *Pst* strains carrying the wild-type or acylation-deficient *avrPphB* alleles. Inoculation of resistant plants with the *Pst*(*avrPphB*) strain results in a *PBS1*-dependent 5-fold increase in *PR1* gene expression relative to mock-treated plants; however, delivery of the acylation-deficient double mutant by *Pst* results in *PR1* induction levels that are equivalent to those generated by the virulent *Pst*(empty vector) strain (Fig. 6*F*). These data indicate that acylation of AvrPphB is essential for up-regulation of *PR1* transcript. Using a variety of genetic and biochemical approaches to examine multiple aspects of the AvrPphB resistance response, we have unambiguously shown that host acylation of AvrPphB drives cleavage of PBS1 and subsequent HR induction in the plant cell.

DISCUSSION

Phytopathogens inject an arsenal of type III effectors into the host cell to thwart defenses and promote disease; however, the molecular strategies that are employed by effectors to target plant signaling components remain largely unknown. Here, we demonstrated that four effectors from the AvrPphB family of cysteine proteases possess a unique autoproteolytic processing activity. Self-cleavage, in turn, reveals embedded consensus sites for eukaryotic acylation. We demonstrated that AvrPphB, ORF4, and NopT are indeed *N*-myristoylated, as well as *S*-palmitoylated by the eukaryotic host machinery, consequently directing them to the plasma membrane (Fig. 7). Furthermore, host-dependent acylation of AvrPphB is necessary for its avirulence activity, and it is likely that lipidation of ORF4 and NopT is indispensable for their function as well. We have also shown that RipT, HopC1, and HopN1 are not lipidated by the host machinery; however, they are nonetheless, directed to the plasma membrane where they likely disrupt host defense signaling networks (Fig. 7). Although the molecular targets of ORF4, NopT, and RipT are unknown, it is possible that substrate specificity can be partially inferred from the amino acid context of the autoprocessing sites. For example, autoprocessing of AvrPphB, as well as cleavage of PBS1, occurs proximal to a GDK motif, suggesting that it may be possible to define the substrate specificities, and putative molecular targets, for ORF4, NopT, and RipT based on the three residues that we identified as essential for autoprocessing (Fig. 7). However, bioinformatic approaches to identify specific *in planta* substrates for these effectors are restricted by the size and chemical makeup of the autoprocessing motif and additional information about the autoprocessing specificity will be required to generate an experimentally testable substrate pool.

We propose that autoprocessing of AvrPphB, ORF4, NopT, and RipT occurs within the plant cell following delivery of the full-length proteins through the TTSS. Supporting this hypothesis, we identified key signatures of the type III secretion signal within the full-length effector sequences but not the autoprocessed sequences (31, 32). Additionally, we observed preferential secretion of the full-length AvrPphB protein by *Pst* grown in culture. Autoprocessing, however, does not exclusively occur within the plant cell because we observed self-cleavage of these effectors in *E. coli*, indicating that a eukaryotic activator is not required for this activity. Therefore, these proteins comprise an effector protease family unique to phytopathogens that is mechanistically distinct from the only other biochemically validated cysteine protease effector AvrRpt2, which requires modification by the eukaryotic peptidyl-prolyl isomerase cyclophilin for activation and subsequent self-processing (33). Surprisingly, two effectors, HopC1 and HopN1, were not capable of self-proteolysis. Although protease activity has yet to be ascribed to HopC1, HopN1 possess *in vitro* protease activity, as well as HR suppression activity in tobacco, both of which require the catalytic triad (34). These two effectors therefore represent an evolutionary distinct non-processing, yet catalytically active, class of cysteine protease effectors within the AvrPphB family.

We clearly demonstrated that autoprocessing of AvrPphB, ORF4, and NopT results in fatty acylation of these effectors by the eukaryotic lipidation machinery. Interestingly, these three autoprocessed effectors, but not RipT, are predicted to be myristoylated using a variety of eukaryotic prediction models (28, 35, 36), suggesting that these bacterially generated acylation sites have been engineered to conform to the restraints of the plant acylation machinery. It is possible that myristoylation of additional AvrPphB family members can be predicted according to these parameters using the following generalized consensus motif: GX_2XXS, where X_2 is a non-acidic residue. Furthermore, genetic experiments suggest that additional effectors

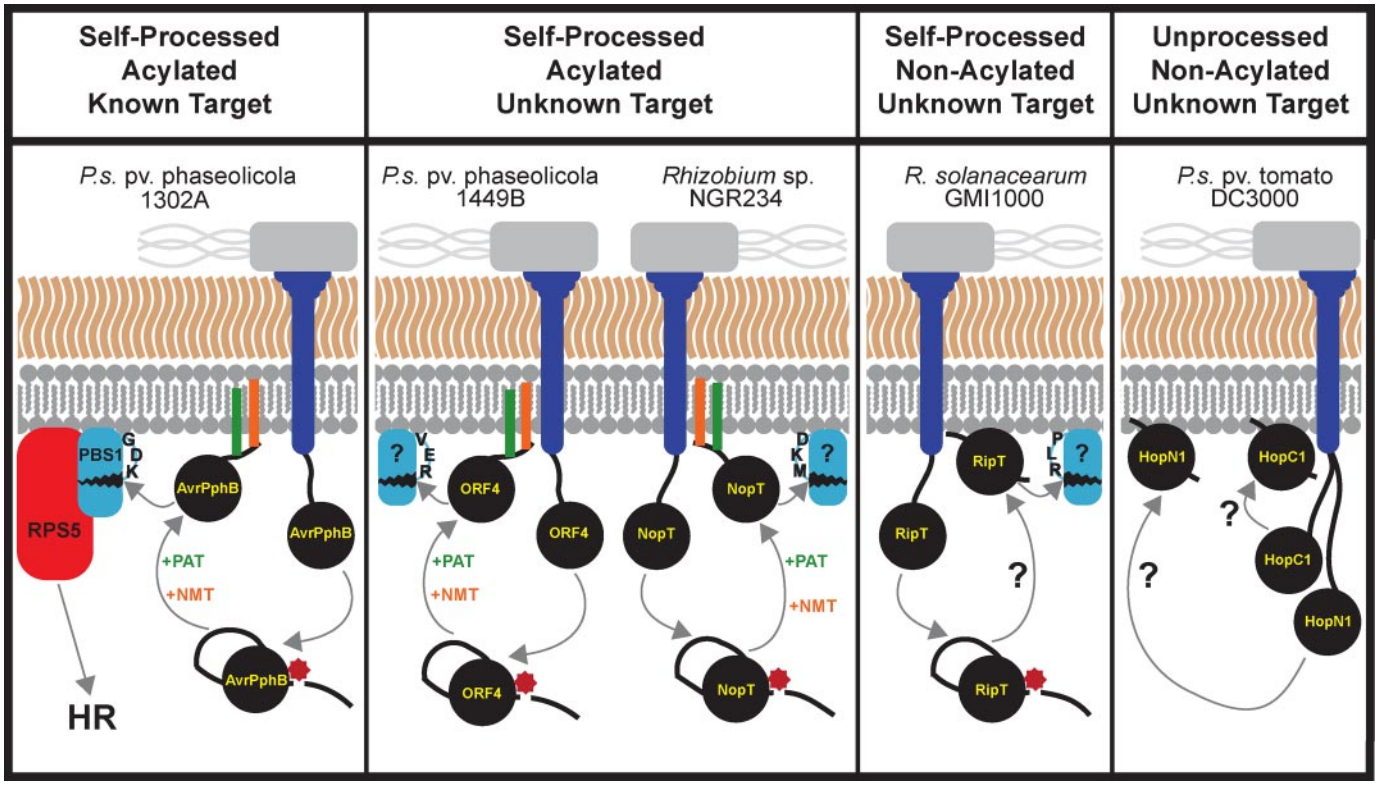

FIGURE 7. **A model for the subcellular localization strategies of the AvrPphB-like effector proteins in the plant cell.** The indicated strains are shown in *gray*, the TTSS in *purple*, and the effectors in *black*. Effectors are classified according to their ability to self-proteolytically process (*red star* in model), to be acylated by the host (*N*-myristoylation, *orange*; *S*-palmitoylation, *green*), and their biological function. AvrPphB, ORF4, and NopT are lipidated by the host machinery (*NMT*, *N*-myristoyl transferase; *PAT*, palmitoyl acyltransferase), whereas RipT, HopC1, and HopN1 are directed to the PM by an unknown mechanism. Host acylation of AvrPphB is essential for cleavage of PBS1 (*blue*) and initiation of RPS5 (*red*) defenses. Unknown targets of ORF4, NopT, and RipT are also included (*blue*) and contain putative target sequences.

may be acylated by the host machinery including AvrPto (37), HopF2 (38), XopE1/XopE2/XopJ (39), and multiple HopZ alleles (40), whereas several more contain putative consensus sites for acylation (41). Prior to our study, however, *in vivo* biochemical evidence supporting host-dependent acylation of effector proteins was limited to *N*-myristoylation of only two *P. syringae* effectors, AvrRpm1 and AvrB (10). We have identified three additional effectors that are myristoylated *in vivo* and have provided the first direct biochemical evidence for modification of effectors by *S*-palmitoylation. Although an overwhelming majority of protein myristoylation is believed to occur co-translationaly at the ribosome where *N*-myristoyltransferases are enriched (42), there is compelling evidence for non-ribosomally associated myristoylation: the mammalian protein BID is myristoylated at an embedded acylation site following proteolytic cleavage by caspase 8 (43). Therefore, the AvrPphB-like effectors are likely myristoylated independently of the ribosome-associated *N*-myristoyltransferases, resulting in a weak plasma membrane association that can be fully stabilized through *S*-palmitoylation of the effectors by plasma membrane-localized palmitoyltransferases (44, 45). Additionally, palmitoylation is a reversible lipid modification that can be dynamically regulated in the eukaryotic cell. We suspect that active depalmitoylation of the acylated effectors by acyl-protein thioesterases *in planta* would likely disrupt the effector-membrane associations and attenuate function.

Previous studies examining the role myristoylation plays in promoting the avirulence function of AvrPphB have provided somewhat conflicting results (10, 46). Nimchuk and colleagues (10) demonstrated that the putative myristoylation site in AvrPphB is required for maximal induction of HR when transiently expressed in *Arabidopsis*; however, an AvrPphB myristoylation-independent HR has also been observed in different plant species using *Agrobacterium* and viral overexpression systems (46). Although it is possible that there are host-specific differences in R protein recognition of AvrPphB, it seems likely that overexpression of AvrPphB results in loss of the myristoylation dependence due to high protein concentrations in the plant cell. We have also observed this phenomenon in transgenic *Arabidopsis* plants overexpressing the AvrPphB acylation-deficient mutant. We delivered AvrPphB and the mutant proteins at near endogenous levels by exogenously expressing the alleles under control of their native promoters in *Pst*, and found an absolute requirement for host acylation of AvrPphB to promote the avirulence function in *Arabidopsis*. Consistent with our results, delivery of AvrPphB using the *P. syringae* pv. *phaseolicola* R6 strain induces HR in bean pods in a myristoylation-dependent manner (46). Interestingly, a recent report demonstrated a NopT acylation-independent HR when the G50A myristoylation mutant was overexpressed in tobacco (47). Our data suggest that delivery of the NopT G50A

mutant at endogenous levels may provide additional insight into the function of the Gly-50 residue.

Type III effectors are likely secreted at low concentrations relative to host signaling molecules, and therefore require a potent, but specific biochemical activity that may be enhanced by increasing the effectors' local concentrations via subcellular localization. We have identified six additional bacterial effectors, including AvrPphB, which localize to host plasma membranes. Although some AvrPphB family members utilize the host lipidation machinery to direct their association with plasma membranes, we demonstrated that others employ acylation-independent plasma membrane localization mechanisms. There are myriad examples of membrane proteins that lack lipid modifications and localize via protein-protein interactions, phospholipid-protein (electrostatic) interactions, or hydrophobic (integral membrane) associations (29). Although the molecular targets of the AvrPphB-like effectors are completely unknown, localization of these effectors to the plasma membrane likely restricts the host substrate pool to co-localizing plasma membrane proteins. An overwhelming amount of evidence has implicated the plasma membrane as a crucial site for initiation of both basal and *R* gene-mediated defenses (48). Mediators of basal defense pathways are often plasma membrane-localized pattern-recognition receptors and include FLS2, EFR, and BAK1, which are all targeted by the plasma membrane-localized effector AvrPto to promote virulence (49, 50). Therefore, plasma membrane-associated R proteins and pattern-recognition receptors, as well as their associated signaling molecules, all serve as possible virulence targets for the AvrPphB family members. The mechanisms that drive type III effector function are only beginning to be unraveled; however, our findings provide critical insight into the diverse subcellular localization mechanisms employed by AvrPphB family members and illustrate the convoluted subversion strategies utilized by the bacterial pathogen.

Acknowledgments—We thank Drs. Brian Staskawicz, James Alfano, Timothy Denny, Maarten Chrispeels, and Richard Kolodner for strains and reagents. We thank Dr. Joshua Gendron, Dr. Hong Qiao, and members of the Ecker and Dixon laboratories for helpful discussions and technical assistance. We are also grateful to Drs. David Pagliarini and Fred Robinson for critical review of this manuscript.

REFERENCES

1. Mackey, D., and McFall, A. J. (2006) *Mol. Microbiol.* **61,** 1365–1371
2. Jones, J. D., and Dangl, J. L. (2006) *Nature* **444,** 323–329
3. Chang, J. H., Urbach, J. M., Law, T. F., Arnold, L. W., Hu, A., Gombar, S., Grant, S. R., Ausubel, F. M., and Dangl, J. L. (2005) *Proc. Natl. Acad. Sci. U. S. A.* **102,** 2549–2554
4. Roine, E., Wei, W., Yuan, J., Nurmiaho-Lassila, E. L., Kalkkinen, N., Romantschuk, M., and He, S. Y. (1997) *Proc. Natl. Acad. Sci. U. S. A.* **94,** 3459–3464
5. Scheel, D. (1998) *Curr. Opin. Plant Biol.* **1,** 305–310
6. Nimchuk, Z., Eulgem, T., Holt, B. F., 3rd, and Dangl, J. L. (2003) *Annu. Rev. Genet.* **37,** 579–609
7. Deslandes, L., Olivier, J., Peeters, N., Feng, D. X., Khounlotham, M., Boucher, C., Somssich, I., Genin, S., and Marco, Y. (2003) *Proc. Natl. Acad. Sci. U. S. A.* **100,** 8024–8029
8. Dodds, P. N., Lawrence, G. J., Catanzariti, A. M., Teh, T., Wang, C. I., Ayliffe, M. A., Kobe, B., and Ellis, J. G. (2006) *Proc. Natl. Acad. Sci. U. S. A.* **103,** 8888–8893
9. Jia, Y., McAdams, S. A., Bryan, G. T., Hershey, H. P., and Valent, B. (2000) *EMBO J.* **19,** 4004–4014
10. Nimchuk, Z., Marois, E., Kjemtrup, S., Leister, R. T., Katagiri, F., and Dangl, J. L. (2000) *Cell* **101,** 353–363
11. Shao, F., Golstein, C., Ade, J., Stoutemyer, M., Dixon, J. E., and Innes, R. W. (2003) *Science* **301,** 1230–1233
12. Shao, F., Merritt, P. M., Bao, Z., Innes, R. W., and Dixon, J. E. (2002) *Cell* **109,** 575–588
13. Ade, J., DeYoung, B. J., Golstein, C., and Innes, R. W. (2007) *Proc. Natl. Acad. Sci. U. S. A.* **104,** 2531–2536
14. Holt, B. F., 3rd, Belkhadir, Y., and Dangl, J. L. (2005) *Science* **309,** 929–932
15. Puri, N., Jenner, C., Bennett, M., Stewart, R., Mansfield, J., Lyons, N., and Taylor, J. (1997) *Mol. Plant-Microbe Interact.* **10,** 247–256
16. Perret, X., Broughton, W. J., and Brenner, S. (1991) *Proc. Natl. Acad. Sci. U. S. A.* **88,** 1923–1927
17. Wang, X., Li, X., Meisenhelder, J., Hunter, T., Yoshida, S., Asami, T., and Chory, J. (2005) *Dev. Cell.* **8,** 855–865
18. Bisgrove, S. R., Simonich, M. T., Smith, N. M., Sattler, A., and Innes, R. W. (1994) *Plant Cell* **6,** 927–933
19. Jamir, Y., Guo, M., Oh, H. S., Petnicki-Ocwieja, T., Chen, S., Tang, X., Dickman, M. B., Collmer, A., and Alfano, J. R. (2004) *Plant J.* **37,** 554–565
20. Simonich, M. T., and Innes, R. W. (1995) *Mol. Plant-Microbe Interact.* **8,** 637–640
21. Warren, R. F., Merritt, P. M., Holub, E., and Innes, R. W. (1999) *Genetics* **152,** 401–412
22. Song, J., Hirschman, J., Gunn, K., and Dohlman, H. G. (1996) *J. Biol. Chem.* **271,** 20273–20283
23. Tornero, P., and Dangl, J. L. (2001) *Plant J.* **28,** 475–481
24. Huynh, T. V., Dahlbeck, D., and Staskawicz, B. J. (1989) *Science* **245,** 1374–1377
25. Nobuta, K., Okrent, R. A., Stoutemyer, M., Rodibaugh, N., Kempema, L., Wildermuth, M. C., and Innes, R. W. (2007) *Plant Physiol.* **144,** 1144–1156
26. Altschul, S. F., Madden, T. L., Schaffer, A. A., Zhang, J., Zhang, Z., Miller, W., and Lipman, D. J. (1997) *Nucleic Acids Res.* **25,** 3389–3402
27. Zhu, M., Shao, F., Innes, R. W., Dixon, J. E., and Xu, Z. (2004) *Proc. Natl. Acad. Sci. U. S. A.* **101,** 302–307
28. Utsumi, T., Sato, M., Nakano, K., Takemura, D., Iwata, H., and Ishisaka, R. (2001) *J. Biol. Chem.* **276,** 10505–10513
29. Resh, M. D. (1999) *Biochim. Biophys. Acta.* **1451,** 1–16
30. Delaney, T. P., Uknes, S., Vernooij, B., Friedrich, L., Weymann, K., Negrotto, D., Gaffney, T., Gut-Rella, M., Kessmann, H., Ward, E., and Ryals, J. (1994) *Science* **266,** 1247–1250
31. Guttman, D. S., Vinatzer, B. A., Sarkar, S. F., Ranall, M. V., Kettler, G., and Greenberg, J. T. (2002) *Science* **295,** 1722–1726
32. Petnicki-Ocwieja, T., Schneider, D. J., Tam, V. C., Chancey, S. T., Shan, L., Jamir, Y., Schechter, L. M., Janes, M. D., Buell, C. R., Tang, X., Collmer, A., and Alfano, J. R. (2002) *Proc. Natl. Acad. Sci. U. S. A.* **99,** 7652–7657
33. Coaker, G., Falick, A., and Staskawicz, B. (2005) *Science* **308,** 548–550
34. Lopez-Solanilla, E., Bronstein, P. A., Schneider, A. R., and Collmer, A. (2004) *Mol. Microbiol.* **54,** 353–365
35. Bologna, G., Yvon, C., Duvaud, S., and Veuthey, A. L. (2004) *Proteomics* **4,** 1626–1632
36. Podell, S., and Gribskov, M. (2004) *BMC Genomics* **5,** 37
37. Shan, L., Thara, V. K., Martin, G. B., Zhou, J. M., and Tang, X. (2000) *Plant Cell* **12,** 2323–2338
38. Robert-Seilaniantz, A., Shan, L., Zhou, J. M., and Tang, X. (2006) *Mol. Plant-Microbe Interact.* **19,** 130–138
39. Thieme, F., Szczesny, R., Urban, A., Kirchner, O., Hause, G., and Bonas, U. (2007) *Mol. Plant-Microbe Interact.* **20,** 1250–1261
40. Lewis, J. D., Abada, W., Ma, W., Guttman, D. S., and Desveaux, D. (2008) *J. Bacteriol.* **190,** 2880–2891
41. Maurer-Stroh, S., and Eisenhaber, F. (2004) *Trends Microbiol.* **12,** 178–185
42. Glover, C. J., Hartman, K. D., and Felsted, R. L. (1997) *J. Biol. Chem.* **272,** 28680–28689
43. Zha, J., Weiler, S., Oh, K. J., Wei, M. C., and Korsmeyer, S. J. (2000) *Science*

290, 1761–1765
44. Berthiaume, L., and Resh, M. D. (1995) *J. Biol. Chem.* **270,** 22399–22405
45. Dunphy, J. T., Greentree, W. K., Manahan, C. L., and Linder, M. E. (1996) *J. Biol. Chem.* **271,** 7154–7159
46. Tampakaki, A. P., Bastaki, M., Mansfield, J. W., and Panopoulos, N. J. (2002) *Mol. Plant-Microbe Interact.* **15,** 292–300
47. Dai, W. J., Zeng, Y., Xie, Z. P., and Staehelin, C. (2008) *J. Bacteriol.* **190,** 5101–5110
48. Nurnberger, T., Brunner, F., Kemmerling, B., and Piater, L. (2004) *Immunol. Rev.* **198,** 249–266
49. Shan, L., He, P., Li, J., Heese, A., Peck, S. C., Nurnberger, T., Martin, G. B., and Sheen, J. (2008) *Cell Host Microbe* **4,** 17–27
50. Xiang, T., Zong, N., Zou, Y., Wu, Y., Zhang, J., Xing, W., Li, Y., Tang, X., Zhu, L., Chai, J., and Zhou, J. M. (2008) *Curr. Biol.* **18,** 74–80